Microscopic Protonation Equilibria of Poly(amidoamine) Dendrimers from Macroscopic Titrations

Dusko Cakara, Jörg Kleimann, and Michal Borkovec*

Department of Inorganic, Analytical, and Applied Chemistry, University of Geneva, 30 Quai Ernest-Ansermet, 1211 Geneva 4, Switzerland

Received January 13, 2003; Revised Manuscript Received April 2, 2003

ABSTRACT: Poly(amidoamine) (PAMAM) dendrimers of generations G0, G1, G2, G3, G4, and G6 are investigated by potentiometric (acid−base) titrations. The data are interpreted with a site binding model, which offers the possibility to model the titration curves for all generations of the dendrimers and to describe all dendrimers within a common parameter set. These parameters involve the microscopic ionization constants for each group in the fully deprotonated state and nearest-neighbor pair interaction parameters. From this model we can further obtain all microscopic ionization constants as well as conditional microstate probabilities. The protonation of PAMAM dendrimers first involves protonation of primary amine groups at the outer rim of the dendrimer at high pH, while the tertiary amine groups in the dendrimer core protonate at lower pH. The last group to protonate at low pH is a central tertiary amine.

1. Introduction

Since their discovery in the late 1970s, dendrimers give much impetus for research because of their unique properties as well as their potential applications as metal complexing agents,[1,2] nanoreactors for particle synthesis,[3] light harvesting devices,[1] or as gene vectors.[5,6] Their unusual properties have been studied by numerous authors.[7−20] Their conformation has been investigated in solution mainly by scattering[7−9] and spectroscopic methods,[10,11] while in the adsorbed state on surfaces with AFM[12] and reflectometry.[13] Their charging behavior was studied by electrochemical techniques,[14−16] NMR,[17,18] and capillary electrophoresis.[19] From the physicochemical point of view, two types of dendrimers are studied best, namely poly(propyleneimine) (PPI) dendrimers[9,14,15,17,18] and poly(amidoamine) (PAMAM) dendrimers (see Figure 1).[7,8,10−12] In both cases, these dendrimers can accumulate positive charge by protonation of the primary amines at the rim and the tertiary amines in the interior. Their charge is thus pH dependent, whereby they are positively charged at low pH and neutral at high pH.

The microscopic charging mechanism of these dendrimers is not immediately obvious and has prompted quite some discussion in the literature.[10,12,14,15,17,18,21] The charging behavior of PPI dendrimers has been studied in substantial detail by potentiometric titrations[14] and ^{15}N NMR.[17] The conclusion of these studies was that these dendrimers protonate in two steps with an intermediate plateau at a degree of protonation of $^2/_3$. During the first step occurring around pH 10, the odd shells protonate, which includes the outermost primary amine groups and the odd shells of tertiary amine groups (i.e., third, fifth, etc.). In the second step around pH 5, the even shells containing the tertiary amine groups protonate (i.e., second, fourth, etc.). Others have suggested that in the PPI dendrimers the primary and tertiary amines protonate almost independently, leading to two distinct protonation steps.[15] Since in a larger dendrimer the numbers of primary and tertiary amine groups are almost the same, this model would incorrectly predict an intermediate plateau at $^1/_2$ and not at $^2/_3$ as observed experimentally.

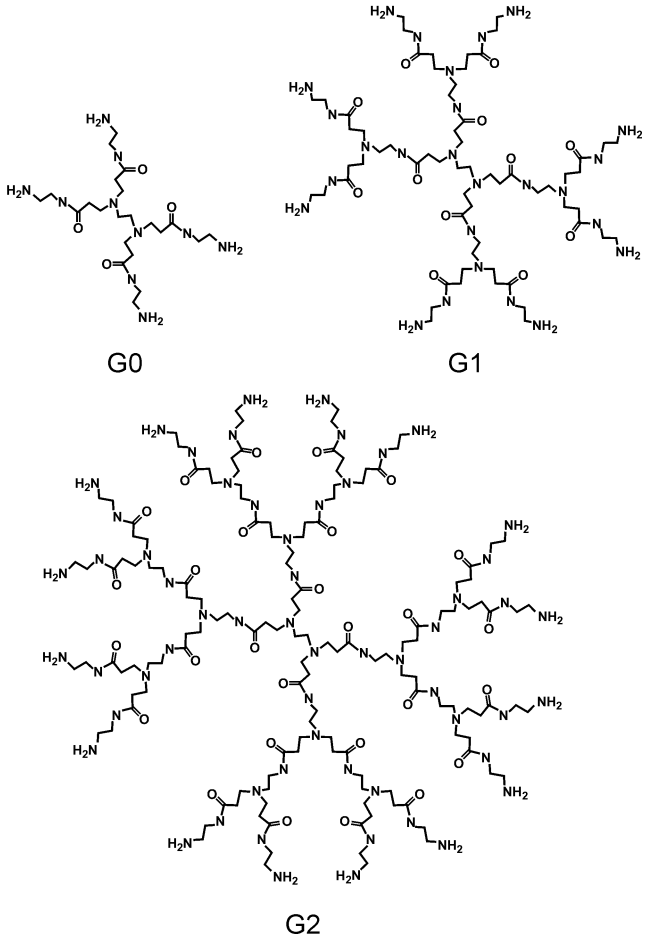

Figure 1. Chemical structure of the poly(amidoamine) (PAMAM) dendrimers for generations G0, G1, and G2.

The charging mechanism of PAMAM dendrimers was suggested to involve two independent protonation steps

* Corresponding author.

10.1021/ma0300241 CCC: $25.00 © 2003 American Chemical Society
Published on Web 04/29/2003

of the primary and tertiary amine groups,[21] while others have surmised that PPI and PAMAM dendrimers should protonate similarly.[12] We shall demonstrate that the protonation mechanism of PAMAM dendrimers is very different from the PPI dendrimers and for higher generations indeed involves the almost independent protonation of primary and tertiary groups, which is consistent with the observed intermediate plateau at $^1/_2$. However, this picture is only partially correct for lower generations, since the two innermost tertiary groups interact strongly and protonate in two distinct steps. These results are obtained by means of a microscopic site binding model, which is based on a cluster expansion of the free energy of protonation.[14,17,18,22,23] The substantial advantage of this model is the small number of parameters necessary to parametrize the microscopic protonation equilibria. Thus, by analyzing several molecules within the homologous series, we can determine these parameters reliably. Once these parameters are known, we can address the microscopic protonation mechanism of the dendrimers and derive microscopic ionization constants, microstate probabilities, and other microscopic properties.

2. Site Binding Model of Protonation Equilibria

Protonation equilibria of polyprotic acids or bases can be described with a site binding model analogous to the classical Ising model.[14,17,18,22,23] To each protonation site i one assigns a state variable s_i ($i = 1, 2, ..., N$), such that $s_i = 1$ if the site is protonated and $s_i = 0$ if the site is deprotonated. The protonation microstate is then specified by the set of state variables $\{s_1, s_2, ..., s_N\}$, abbreviated as $\{s_i\}$. Neglecting the intermolecular interactions in a dilute solution, the free energy of a particular microstate relative to the fully deprotonated state can be written as an expansion

$$\frac{\beta F(\{s_i\})}{\ln 10} = -\sum_i \mathrm{p}\hat{K}_i s_i + \frac{1}{2}\sum_{i,j} \epsilon_{ij} s_i s_j + ... \qquad (1)$$

where the sums run over all the sites, $\mathrm{p}\hat{K}_i$ is the microscopic ionization constant of the site i given all other sites are deprotonated, and ϵ_{ij} are pair interaction parameters. The pair interactions obey the symmetry relation $\epsilon_{ij} = \epsilon_{ji}$ and $\epsilon_{ii} = 0$. Consideration of higher order interactions is not necessary here. The pair interactions are mainly electrostatic, and their magnitude decreases quickly with increasing distance between the ionizable groups. The set of so-called *cluster parameters* $\mathrm{p}\hat{K}_i$ and ϵ_{ij} fully define the model, and particularly due to symmetry their number can remain moderate even for complex molecules.

The probability of a given microstate can be evaluated as[22,23]

$$p(\{s_i\}) = \Xi^{-1} a_\mathrm{H}^n \mathrm{e}^{-\beta F(\{s_i\})} \qquad (2)$$

where we have introduced the activity of protons a_H (where $\mathrm{pH} = -\log a_\mathrm{H}$), the inverse thermal energy β, the total number of bound protons

$$n = \sum_{i=1}^{N} s_i \qquad (3)$$

and a normalization constant

$$\Xi = \sum_{\{s_i\}} a_\mathrm{H}^n \mathrm{e}^{-\beta F(\{s_i\})} \qquad (4)$$

This normalization constant can be interpreted as a partition function.

The average degree of protonation of an individual site m can be evaluated by averaging the state variable s_m over all microstates, namely

$$\theta_m = \sum_{\{s_i\}} s_m p(\{s_i\}) \qquad (5)$$

The average degree of protonation of the entire molecule can be obtained from the average of all site protonation curves, namely

$$\theta = \frac{1}{N}\sum_{m=1}^{N} \theta_m \qquad (6)$$

This expression can be rewritten in terms of more familiar quantities by realizing that the partition function Ξ given in eq 4 can be expressed as

$$\Xi = \sum_{n=0}^{N} \bar{K}_n a_\mathrm{H}^n \qquad (7)$$

where

$$\bar{K}_n = \sum_{\{s_i\}} \mathrm{e}^{-\beta F(\{s_i\})} \delta_{n,\Sigma_j s_j} \qquad (8)$$

is the cumulative association constant. (The Kronecker symbol is denoted as δ_{ij} with $\delta_{ii} = 1$ and vanishes otherwise.) The commonly used macroscopic stepwise dissociation constants can be expressed in terms of the cumulative constants as $\mathrm{p}K_n = \log \bar{K}_n/\bar{K}_{n-1}$. Equation 7 is also being referred to as the *binding polynomial*. The probability of a particular macrostate is then given by

$$P_n(a_\mathrm{H}) = \Xi^{-1} \bar{K}_n a_\mathrm{H}^n \qquad (9)$$

and the macroscopic titration curve can be expressed as

$$\theta = \frac{a_\mathrm{H}}{N}\frac{\partial \log \Xi}{\partial a_\mathrm{H}} = \frac{1}{N}\sum_{n=0}^{N} n P_n(a_\mathrm{H}) \qquad (10)$$

or equivalently

$$\theta = \frac{1}{N}\frac{\sum_{n=0}^{N} n \bar{K}_n a_\mathrm{H}^n}{\sum_{n=0}^{N} \bar{K}_n a_\mathrm{H}^n} \qquad (11)$$

This function is directly measurable by classical potentiometric titration. Equivalently, by fitting eq 11 to experimental data, all cumulative association constants (or equivalently all macroscopic pK values) can be determined.

Microscopic ionization constants can be calculated once all the cluster parameters $\mathrm{p}\hat{K}_i$ and ϵ_{ij} specifying the microscopic equilibria are known. These ionization constants commonly refer to the protonation reaction, where one particular site is being protonated. If we label

this site with j, the association equilibrium can be written as

$$A\{s_i\} + H \rightleftharpoons A\{s_i'\} \tag{12}$$

where $s_i = s_i'$ for all $i \neq j$ but $s_j = 0$ and $s_j' = 1$. Using the free energy eq 1, the microscopic pK value for the reaction given by eq 12 follows as[23]

$$p\hat{K}_{A\{s_i\}} = p\hat{K}_i - \sum_j \epsilon_{ij} s_j - \dots \tag{13}$$

This relation reflects the group additivity concept for the estimation of pK values.[26] In the present approach, the microconstants represent secondary parameters, which can be easily evaluated once the primary cluster parameters are known.

One can further evaluate the microstate probabilities within a macrostate. The microstate probabilities can be split into a product as

$$p(\{s_i\}) = \pi_n(\{s_i\}) P_n(a_H) \tag{14}$$

where $P_n(a_H)$ is the macrostate probability and $\pi_n(\{s_i\})$ is the conditional probability to find a particular microstate within its macrostate n (cf. eq 3) given by

$$\pi_n(\{s_i\}) = \bar{K}_n^{-1} e^{-\beta F(\{s_i\})} \tag{15}$$

As this quantity is pH-independent, it is easily interpreted as the mole fraction of a particular microstate within a macrostate n.

The cluster parameters can be determined by fitting the macroscopic titration curves based on the site binding model. In contrast to the macroconstants, the number of cluster parameters remains the same for all dendrimer generations. Once these parameters are known, the microconstants and microstate probabilities can be calculated. For moderately sized molecules ($N <$ 25) the model was evaluated numerically by direct enumeration of all states. For larger molecules, the model was also solved exactly employing a transfer matrix technique. A detailed description of this technique is given elsewhere.[24]

3. Experimental Section

The potentiometric titrations were carried out with a Wallingford titrator, which is a fully computer-controlled instrument with four automatic burets containing 0.25 M HCl (Merck Titrisol), 0.25 M CO_2-free KOH (Baker Dilut-It), 3.0 M KCl (Merck, p.a.), and pure water. All solutions were prepared with water from a Milli-Q A10 UV/UF (Millipore) system, from which the residual CO_2 was eliminated through boiling. The double-wall potentiometric plexiglass cell is thermostatized to 25 °C and continuously flushed with moist CO_2-free nitrogen. The potential between a separate glass electrode and an Ag/AgCl reference electrode is measured with an high-impedance voltmeter (Microlink PH4-S) after the drift criterion of <0.1 mV/min has been achieved. Further details on the Wallingford titrator are given elsewhere.[14]

A typical run starts with the titration of acidified solution with KOH and is then back-titrated with HCl. The instrument maintains a constant ionic strength during such a titration. The overall ionic strength of the sample can be increased thereafter. Thus, a whole sequence of acid−base titrations at different ionic strengths can be carried out automatically within a single titration experiment.

Blank titrations are used to calibrate the glass electrode in a pH range between 3 and 11 at ionic strengths in the range 0.1−1.0 M. The exact base concentration and the activity coefficients were determined by a least-squares fit. Starburst polyamidoamine (PAMAM) dendrimers (Dendritech Corp., Midland, MI) are titrated at total concentrations of amine groups of 10 and 20 mM. By taking the difference between the titration curves of the sample and the blank, the charging curve of the dendrimers is obtained. The titration curves are normalized with the known concentration of the dendrimers and reported as the overall degree of protonation θ as a function of pH. The estimated errors are ±0.01 for θ and ±0.02 for pH. The overall performance of the system was checked with titrations of ethylenediamine and acetic acid. The resulting ionization constants were in accord with literature values[25] within the expected error. The dendrimer concentrations were determined from the titration curves and were within 2% of the values expected from the sample dosage.

Table 1. Cluster Parameters of the Site Binding Model of the PAMAM Dendrimers

I (M)	$p\hat{K}^{(I)}$	$p\hat{K}^{(III)}$	$p\hat{K}^{(III')}$	ϵ	ϵ'	Δ
0.1	9.00	6.00	6.70	0.15	2.85	0.14
0.5	9.20	6.50	7.00	0.15	2.85	0.07
1.0	9.30	6.70	7.30	0.15	2.85	0.06

4. Results

Potentiometric titration curves of PAMAM dendrimers at ionic strengths 0.1, 0.5, and 1.0 M in KCl for the different generations G0, G1, G2, G3, G4, and G6 are presented in Figure 2. The solid lines are model calculations to be discussed below. The titration (or charging) curves show the characteristic dependence with the ionic strength for a polybase, which is becoming more acidic with decreasing ionic strength.[14,22] It was further verified that the titration curves were fully reversible and independent of the dendrimer concentration within experimental error, indicating that dendrimer−dendrimer interactions are negligible.

The titration curves undergo a characteristic transition with increasing generation number. This transition is more clearly illustrated in Figure 3, where we plot the titration curves for the different generations at fixed ionic strength of 0.5 M. The smallest dendrimer G0 has six ionizable sites (four primary and two tertiary amine groups; see Figure 1 and Table 1) and shows three protonation steps and two intermediate plateaus at $\theta = {}^4/_6$ and ${}^5/_6$. On the other hand, the largest dendrimer G6 with 510 ionizable sites shows two protonation steps and an intermediate plateau at $\theta = {}^1/_2$. The differences between titration curves of the smaller dendrimers are substantial, while the titration curves of the dendrimers G4 and above are minor and reflect the large molecule limit. This limit, where the titration curves becomes independent of molecular weight, is characteristic for polyelectrolytes.

Modeling and Interpretation. The experimental data have been quantified in two different ways. First, by describing them in the classical way in terms of macroscopic equilibria and, second, by using the site binding model presented in section 2.

Determination of Macroconstants. The macroscopic ionization constants have been determined by a least-squares fit of the experimental titration curve (cf. eq 11). The resulting macroconstants pK_n are summarized in Tables 2 and 3. For G0 there were six constants determined, while for G1 there are 14. While these numbers can be obtained with reasonable confidence, this classical picture has two disadvantages. First of all, it becomes impractical with increasing generation number, as the number of macroconstants increases quickly. Furthermore, it does not lead to insight into

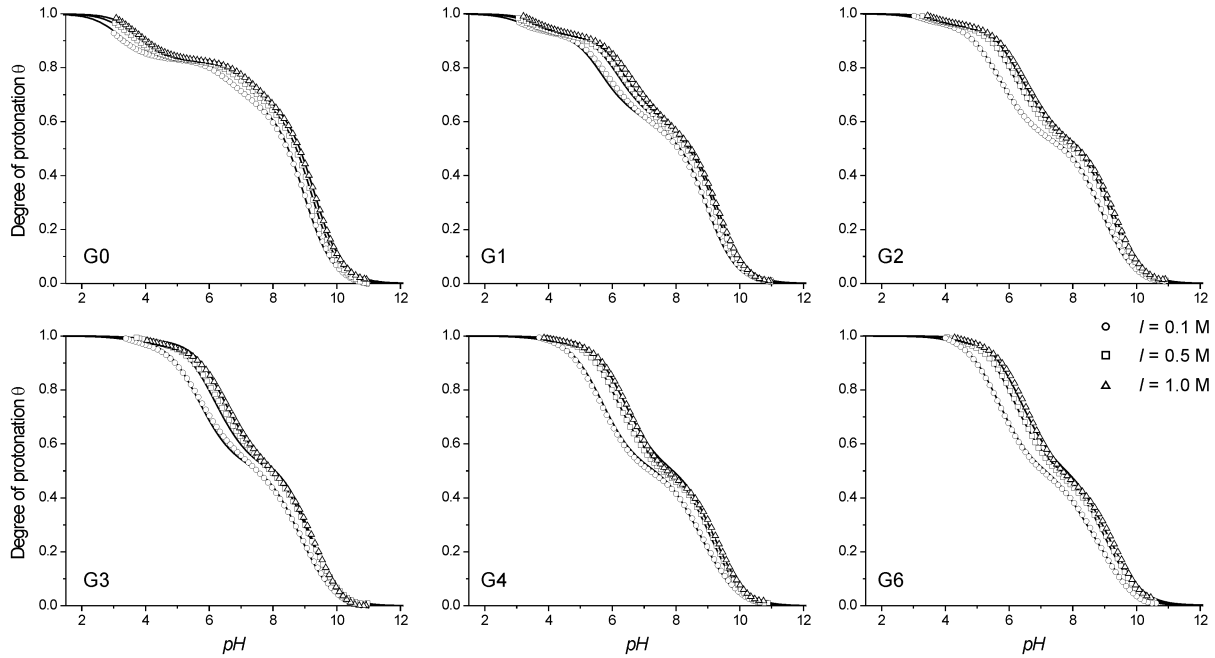

Figure 2. Potentiometric titration curves at different ionic strengths in KCl of PAMAM dendrimers of generations G0, G1, G2, G3, G4, and G6. Solid lines are calculations with the site binding model.

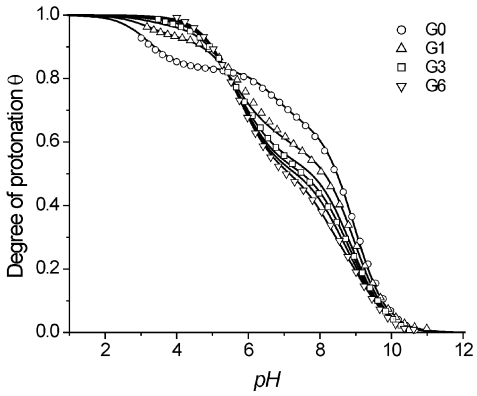

Figure 3. Potentiometric titration curves of PAMAM dendrimers of generations G0, G1, G2, G3, G4, and G6 at at ionic strength 0.5 M in KCl. Solid lines are calculations with the site binding model.

Table 2. Comparison of Macroscopic Ionization Constants pK_n of the PAMAM Dendrimer G0 from Direct Fit of the Titration Curves and Calculated from the Site Binding Model at Different Ionic Strengths

	0.1 M		0.5 M		1.0 M	
n	fit	model	fit	model	fit	model
1	9.70	9.59	9.83	9.78	9.89	9.87
2	9.26	9.17	9.47	9.36	9.55	9.45
3	8.74	8.82	8.99	9.01	9.10	9.10
4	8.31	8.39	8.61	8.59	8.73	8.68
5	6.68	6.67	7.13	7.03	7.34	7.32
6	3.15	3.21	3.65	3.57	3.91	3.87

the microscopic protonation mechanism of the molecule. Both disadvantages can be overcome with the site binding model discussed now.

Site Binding Model. The experimental titration data were further described with the site binding model discussed in section 2. The cluster parameters are illustrated in Figure 4. Since the ionizable amine groups are relatively far apart, we assume pair interactions only. Nearest-neighbor interactions act along bonds, namely one containing the amide bond with an interaction parameter ϵ and the ethyl chain in the center of the dendrimer with an interaction parameter ϵ'. As we shall see, a nonzero next-nearest-neighbor interaction parameter ϵ'' between the primary amine groups must be introduced, similarly as in the description of the charging behavior of carboxylated dendrimers.[16]

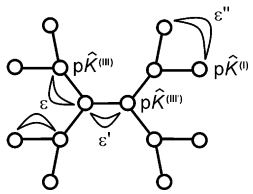

Figure 4. Definition of the cluster parameters of the site binding model. The circles denotes the ionizable amine groups connected with amide links, with the exception of central ethylene links.

Table 3. Comparison of Macroscopic Ionization Constants pK_n of the PAMAM Dendrimer G1 from Direct Fit of the Titration Curves and Calculated from the Site Binding Model at Different Ionic Strengths

	0.1 M		0.5 M		1.0 M	
n	fit	model	fit	model	fit	model
1	9.95	9.85	10.02	10.78	10.16	10.15
2	9.70	9.50	9.87	9.72	9.76	9.79
3	9.25	9.25	9.47	9.47	9.76	9.54
4	9.19	9.05	9.34	9.27	9.28	9.34
5	8.78	8.86	9.08	9.08	9.21	9.15
6	8.68	8.65	8.92	8.88	9.07	8.95
7	8.30	8.41	8.57	8.64	8.60	8.72
8	7.96	8.07	8.29	8.30	8.47	8.39
9	7.10	7.06	7.43	7.44	7.50	7.68
10	6.36	6.35	6.91	6.81	7.21	7.00
11	5.95	5.96	6.33	6.43	6.39	6.61
12	5.55	5.61	6.17	6.08	6.56	6.27
13	5.10	5.18	5.52	5.66	5.59	5.84
14	3.07	3.20	3.51	3.57	3.66	3.86

The microconstant of the primary amine groups is denoted by $p\hat{K}^{(I)}$. For the tertiary groups, two different microconstants must be distinguished due to different chemical environments. The microconstant of the in-

nermost tertiary amines is denoted by $p\hat{K}^{(III')}$, while for all others the same value of $p\hat{K}^{(III)}$ will be used.

While these parameters cannot be uniquely determined from a single titration curve, they can be obtained by a simultaneous fit of G0 and G1 data. The interaction parameters are $\epsilon = 0.15$ and $\epsilon' = 2.85$. At this point we have set $\epsilon'' = 0$. The ionization constants increase with the ionic strength, and the values are given in Table 1. While a slight decrease of the interaction parameters with increasing ionic strength could be found, the data can be equally well described by assuming these parameters to be ionic strength independent. This approach was adopted here for simplicity.

For the dendrimers G2, G3, G4, and G6 we observe that a good fit cannot be obtained without introducing an interaction between the primary amines ϵ''. While the data for all dendrimer generations can be obtained with the same cluster parameters, one further observes that ϵ'' increases with increasing generation number. We have found that this dependence can be modeled as

$$\epsilon'' = \Delta(k - 1) \tag{16}$$

where k is the generation number ($k > 1$) and Δ is ionic strength dependent and is given in Table 1. For G0 and G1 ($k = 0, 1$) we have $\epsilon'' = 0$, and this interaction is negligible. From Figures 2 and 3 one can see that this five-parameter model describes all experimental data at a given ionic strength to good accuracy.

The interaction parameter for the amide bond $\epsilon \simeq 0.15$ has not been reported in the literature before, but its value is well comparable with the corresponding value of 0.18 for an alkyl chain with the corresponding number of carbon atoms, as in hexamethyleneamine.[22] The interaction parameter $\epsilon' \simeq 2.87$ is somewhat larger than the value of 2.13 reported for ethylenediamine.[22] This increase is probably caused by the presence of the amido side chains coordinating the nitrogen atoms. Note that ϵ'' decreases within increasing ionic strength, while ϵ and ϵ' are virtually ionic strength independent. This difference can be understood by realizing that the nearest-neighbor interactions parametrized by ϵ and ϵ' act mainly along the hydrocarbon backbone, while the interactions between the primary amines parametrized by ϵ'' act through the solution, and thus one observes stronger effects of the ionic strength due to effects of screening.[20,22] The trend in the increase of ϵ'' with the generation number is similar to the sequence of conformations observed by small-angle scattering.[8] The negligible interaction between the primary amine groups for G0 and G1 reflects the open structure of these denrimers, while its increase for higher generations is in line with the increasingly compact structure of the larger dendrimers.

The microscopic ionization constants of the amine groups are generally lower than the corresponding values for aliphatic amines but show the same trends otherwise. For primary amine groups, $p\hat{K}^{(I)}$ in the range 9.4−9.7 has been reported, while for tertiary amine groups $p\hat{K}^{(III)}$ lies around 7.5.[22]

As shown in Tables 2 and 3, the site binding model can equally well predict the fitted macroconstants pK_n obtained from eq 8. This feature illustrates that the classical description in terms of the macroscopic equilibria is inherent to the site binding model. In contrast to the classical picture, however, the site binding model is capable of quantifying the protonation behavior within an entire homologous series with a limited number of parameters.

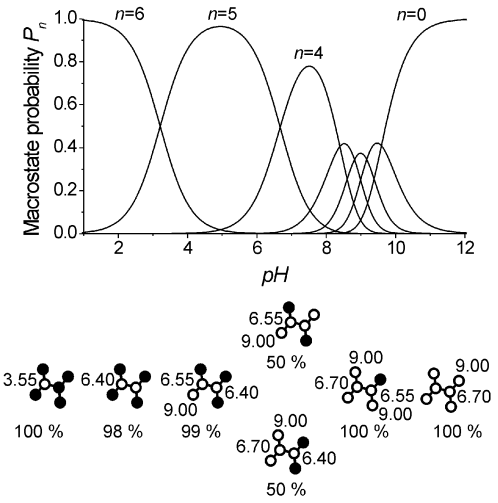

Figure 5. Microscopic protonation mechanism for the PAMAM dendrimer G0: (top) macrostate probabilities as a function of pH; (bottom) microstate probabilities and microconstants.

Microscopic Protonation Mechanism. With the site binding model one can further address the microscopic protonation mechanism in detail. Once the model parameters have been determined, we can calculate the site-specific titration curves, microstate probabilities, and all microconstants (cf. eq13). Let us now illustrate these results for dendrimers G0 and G1 in detail and then qualitatively discuss the microscopic protonation mechanism of the large dendrimers. For illustration purposes, we consider the results at an ionic strength 0.1 M.

Figure 5 illustrates the microscopic protonation mechanism of dendrimer G0. The macrostate probabilities are illustrated in Figure 5a, and the microstates with the corresponding conditional probabilities and microconstants are given in Figure 5b.

The microscopic protonation pattern can be described as follows. The primary amines protonate independently with a microscopic ionization constant $pK^{(I)} \simeq 9.00$. A prominent state is formed when all primary amine groups are protonated and both tertiary amines deprotonated ($n = 4$). This species reflects the plateau at $\theta = {}^4/_6$ in the macroscopic titration curve. When decreasing the pH further, one tertiary group protonates. This process is controlled by the microscopic ionization constant $p\hat{K}^{(III')} - 2\epsilon \simeq 6.40$ and leads to the microstate where all primary groups and one tertiary groups are protonated ($n = 5$). The plateau at $\theta = {}^5/_6$ in the macroscopic titration curve reflects this species. The final protonation step is controlled by the microconstant $p\hat{K}^{(III')} - 2\epsilon - \epsilon' \simeq 3.55$.

Figure 6 illustrates the microscopic protonantion mechanism of dendrimer G1. Again, Figure 6a shows the macrostate probabilities and Figure 6b the most probable microstates. The microscopic protonation pattern is now somewhat more complicated, but the trends are similar to the G0 dendrimer. All primary groups protonate independently with a microconstant $pK^{(I)} \simeq 9.00$, leading to a prominent microstate where all primary groups are protonated ($n = 8$). The next protonation step mainly involves the protonation of the innermost tertiary amine and is controlled by the microconstant $p\hat{K}^{(III')} \simeq 6.70$. With the exception of the other central tertiary amine group, the remaining

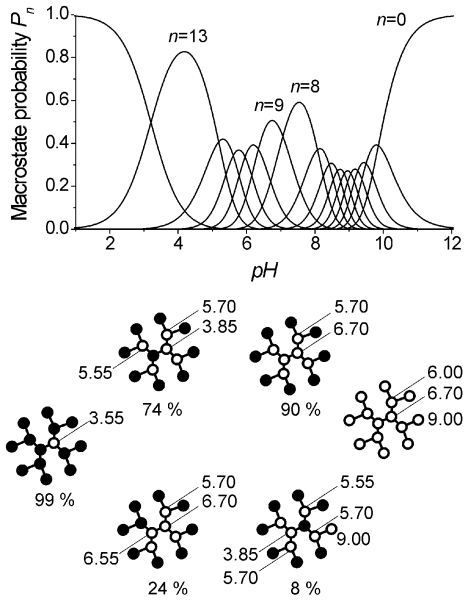

Figure 6. Microscopic protonation mechanism for the PAMAM dendrimer G1: (top) macrostate probabilities as a function of pH; (bottom) microstate probabilities and microconstants.

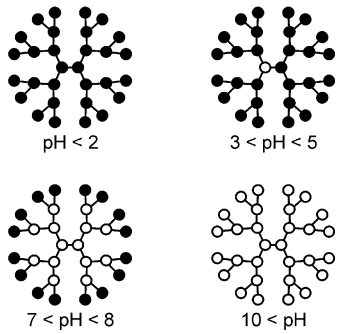

Figure 7. Schematic microscopic protonation mechanism for a large PAMAM dendrimer.

groups protonate almost independently, as this process is controlled by two very similar microconstants, namely $pK^{(III)} - 2\epsilon \simeq 5.70$ and $pK^{(III)} - 3\epsilon \simeq 5.55$. Once this process is terminated, one obtains a prominent microspecies where all amine groups are protonated with the exception of one central tertiary group. In this configuration, this group has a microcostant of $pK^{(III')} - 2\epsilon - \epsilon' \simeq 3.55$, and its protonation controls the last protonation step.

With these results at hand, we can propose a protonation mechanism of a large dendrimer, as illustrated in Figure 7. In the first protonation step, the primary amines will protonate independently with a microconstant $pK^{(I)}$ around 9.0. The result is a stable microspecies where all primary amines are protonated and all tertiary amines deprotonated, which leads to the intermediate plateau of the macroscopic titration curve close to $\theta = {}^1/_2$. The tertiary groups protonate almost independently with a microconstant around 5.8. This process leads to the stable microspecies where all groups are protonated, with the exception of one central tertiary group. This group has a microcostant around 3.5. For large dendrimers, however, this last protonation step contributes very little to the overall charge.

This protonation pattern is rather distinct from the charging behavior of poly(propyleneimine) (PPI) dendrimers.[14,17] While the ionizable groups in these dendrimers are also primary and tertiary groups, there are two main differences with respect to their protonation behavior. The first difference concerns the distance between the amine groups, which is much smaller in the PPI dendrimers, and thus their mutual interactions are stronger and play a much more important role than in the PAMAM dendrimers. The second difference concerns the microscopic ionization constants of the primary and tertiary amine groups. While the tertiary groups are more acidic than the primary groups in both types of dendrimers, the differences between the proton affinities of these two groups is substantial. While these values are rather comparable in the PPI dendrimers, they lie rather far apart in the PAMAM dendrimers. These features lead to the characteristic onionlike protonation pattern for the PPI dendrimers. In a first protonation step, not only the primary amines protonate but also all tertiary amines residing in odd shells. This process leads to a stable microstate, where all odd shells are being protonated, and causes an intermediate plateau at $\theta = {}^2/_3$. In the second step, the tertiary amine groups in the even shells protonate. This picture has been derived from potentiometric titrations[14] and confirmed with ^{15}N NMR.[17]

5. Conclusion

Poly(amidoamine) (PAMAM) dendrimers of generations G0, G1, G2, G3, G4, and G6 were investigated by potentiometric titrations, and the data were analyzed in terms of classical macroscopic protonation equilibria and a site binding model. While both descriptions are equivalent, the site binding model offers further the possibility to model the titration curves of the higher generation dendrimers and to describe all dendrimers within a common set of parameters. These parameters involve the microscopic ionization constants for each group in the fully deprotonated state and nearest-neighbor pair interaction parameters. On the basis of this parametrization of the site binding model, we can predict all microscopic ionization constants as well as conditional microstate probabilities.

From this analysis we deduce the following microscopic protonation mechanism of PAMAM dendrimers. At high pH, the primary amine groups at the outer rim of the dendrimer protonate, while the tertiary amine groups in the dendrimer core only protonate at lower pH. The last group to protonate is one of the central tertiary amine groups. This study demonstrates that by analyzing macroscopic titration data of a homologous series of polyprotic molecules the detailed information about microscopic protonation equilibria can be obtained.

Acknowledgment. This work has been supported by the Swiss National Science Foundation (Grant 2100-066514.01).

References and Notes

(1) Vögtle, F.; Gestermann, S.; Hesse, R.; Schwierz, H.; Windisch, B. *Prog. Polym. Sci.* **2000**, *25*, 987−1041.

(2) Sun, L.; Crooks, R. M. *J. Phys. Chem. B* **2002**, *106*, 5864−5872.

(3) Ottaviani, M. F.; Valluzzi, R.; Balogh, L. *Macromolecules* **2002**, *35*, 5105−5115.

(4) Yamamoto, K.; Higuchi, M.; Shiki, S.; Tsuruta, M.; Chiba, H. *Nature (London)* **2002**, *415*, 509−511.

(5) Haensler, J.; Szoka, F. C. *Bioconjugate Chem.* **1993**, *4*, 372−379.

(6) Kukowska-Latallo, J. F.; Bielinska, A. U.; Johnson, J.; Spindler, R.; Tomalia, D. A.; Baker, J. R. *Proc. Natl. Acad. Sci U.S.A.*. **1996**, *93*, 4897−4902.
(7) Prosa, T. J.; Bauer, B. J.; Amis, E. J. *Macromolecules* **2001**, *34*, 4897−4906.
(8) Nisato, G.; Ivkov, R.; Amis, E. J. *Macromolecules* **2000**, *33*, 4172−4176.
(9) Ramzi, A.; Scherrenberg, R.; Joosten, J.; Lemstra, P.; Mortensen, K. *Macromolecules* **2002**, *29*, 827−833.
(10) Ottaviani, M. F.; Monalti, F.; Romanelli, M.; Turro, N. J.; Tomalia, D. A. *J. Phys. Chem. B* **1996**, *100*, 11033−11042.
(11) Chen, W.; Tomalia, D. A.; Thomas, J. L. *Macromolecules* **2000**, *33*, 9169−9172.
(12) Betley, T. A.; Banaszak Holl, M. M.; Orr, B. G.; Swanson, D. R.; Tomalia, D. A.; Baker, J. R. *Langmuir* **2001**, *17*, 2768−2773.
(13) van Duijvenbode, R. C.; Koper, G. J. M.; Bohmer, M. R. *Langmuir* **2000**, *16*, 7713−7719.
(14) van Duijvenbode, R. C.; Borkovec, M.; Koper, G. J. M. *Polymer* **1998**, *39*, 2657−2664.
(15) Kabanov, V. A.; Zezin, A. B.; Rogacheva, V. B.; Gulyaeva, Z. G.; Zansochova, M. F.; Joosten, J. G. H.; Brackman, J. *Macromolecules* **1998**, *31*, 5142−5144.
(16) van Duijvenbode, R. C.; Rajanayagam, A.; Koper, G. J. M.; Baars, M. W. P. L.; de Waal, B. F. M.; Meijer, E. W.; Borkovec, M. *Macromolecules* **2000**, *33*, 46−52.
(17) Koper, G. J. M.; van Genderen, M. H. P.; Elissen-Roman, C.; Baars, M. W. P. L.; Meijer, E. W.; Borkovec, M. *J. Am. Chem. Soc.* **1997**, *119*, 6512−6521.
(18) Borkovec, M.; Koper, G. J. M. *Anal. Chem.* **2000**, *72*, 3272−3279.
(19) Huang, Q. R.; Dubin, P. L.; Moorefield, C. N.; Newkome, G. R. *J. Phys. Chem. B* **2000**, *104*, 898−904.
(20) Welch, P.; Muthukumar, M. *Macromolecules* **1998**, *31*, 5892−5897.
(21) Lee, I.; Athley, B. D.; Wetzel, A. W.; Meixner, W.; Baker Jr., J. R. *Macromolecules* **2002**, *35*, 4510−4520.
(22) Borkovec, M.; Jönsson, B.; Koper, G. J. M. In *Surface and Colloid Science*; Matijevic, E., Ed.; Kluwer Academic/Plenum Publishers: New York, 2001; Vol. 16.
(23) Borkovec, M.; Koper, G. J. M. *J. Phys. Chem.* **1994**, *98*, 6038.
(24) Borkovec, M.; Koper, G. J. M. *Macromolecules* **1997**, *30*, 2151−2158.
(25) Smith, R. M.; Martell, A. E. *Critical Stability Constants*; Plenum Press: New York, 1989; Vol. 6.
(26) Perrin, D. D.; Dempsey, B.; Serjeant, E. P. pK_a *Prediction for Organic Acids and Bases*; Chapman & Hall: London, 1981.

MA0300241